

Distinct Molecular Profiles and Immunotherapy Treatment Outcomes of V600E and V600K *BRAF*-Mutant Melanoma



Inês Pires da Silva¹, Kevin Y.X. Wang², James S. Wilmott¹, Jeff Holst³, Matteo S. Carlino^{1,4}, John J. Park⁵, Camelia Quek¹, Matthew Wongchenko⁶, Yibing Yan⁶, Graham Mann^{1,7}, Douglas B. Johnson⁸, Jennifer L. McQuade⁹, Rajat Rai¹, Richard F. Kefford^{1,4,5}, Helen Rizos^{1,5}, Richard A. Scolyer^{1,10}, Jean Y.H. Yang², Georgina V. Long^{1,11}, and Alexander M. Menzies^{1,11}

Abstract

Purpose: *BRAF* V600E and V600K melanomas have distinct clinicopathologic features, and V600K appear to be less responsive to *BRAF*±*MEK*i. We investigated mechanisms for this and explored whether genotype affects response to immunotherapy.

Experimental Design: Pretreatment formalin-fixed paraffin-embedded tumors from patients treated with *BRAF*±*MEK*i underwent gene expression profiling and DNA sequencing. Molecular results were validated using The Cancer Genome Atlas (TCGA) data. An independent cohort of V600E/K patients treated with anti-PD-1 immunotherapy was examined.

Results: Baseline tissue and clinical outcome with *BRAF*±*MEK*i were studied in 93 patients (78 V600E, 15 V600K). V600K patients had numerically less tumor regression (median, -31% vs. -52%, $P = 0.154$) and shorter progression-free survival (PFS; median, 5.7 vs. 7.1 months, $P = 0.15$) compared with V600E. V600K melanomas had

lower expression of the ERK pathway feedback regulator dual-specificity phosphatase 6, confirmed with TCGA data (116 V600E, 17 V600K). Pathway analysis showed V600K had lower expression of ERK and higher expression of PI3K-AKT genes than V600E. Higher mutational load was observed in V600K, with a higher proportion of mutations in *PIK3R1* and tumor-suppressor genes. In patients treated with anti-PD-1, V600K ($n = 19$) had superior outcomes than V600E ($n = 84$), including response rate (53% vs. 29%, $P = 0.059$), PFS (median, 19 vs. 2.7 months, $P = 0.049$), and overall survival (20.4 vs. 11.7 months, $P = 0.081$).

Conclusions: *BRAF* V600K melanomas appear to benefit less from *BRAF*±*MEK*i than V600E, potentially due to less reliance on ERK pathway activation and greater use of alternative pathways. In contrast, these melanomas have higher mutational load and respond better to immunotherapy.

Introduction

The identification of *BRAF* driver mutations in melanoma has led to the development of specific inhibitors targeting the ERK pathway, which have high response rates and improve survival in patients with *BRAF*-mutant advanced melanoma and those at high risk of recurrence (1–4). *BRAF* mutations are present in approximately 40% of cutaneous melanomas, and the majority occur at codon 600 (90%; ref. 5). Among these, 70% to 80% are V600E (codon GTG>GAG), 20% to 30% are V600K (GTG>AAG), and rarer mutations including V600R (GTG>AGG), V600D (GTG>GAT), V600E2 (GTG>GAA), V600G (GTG>GGG), V600M (GTG>ATG), V600A (GTG>GCG), and V600L (GTG>TTG; refs. 1, 6, 7).

Previous studies have shown that V600E and V600K *BRAF*-mutant metastatic melanomas have distinct clinicopathologic features, suggesting different etiology (8, 9). V600K melanomas occur more frequently in older people, in the head and neck region, and are associated with chronic sun damage (8, 9). Furthermore, even though individual phase III targeted therapy trials have not performed a direct comparison between V600E and V600K-mutant melanomas, in three separate trials, V600K melanomas had numerically lower response rate and shorter median

¹Melanoma Institute Australia and The University of Sydney, Sydney, New South Wales, Australia. ²School of Mathematics and Statistics, The University of Sydney, Sydney, New South Wales, Australia. ³School of Medical Sciences and Prince of Wales Clinical School, University of New South Wales, Sydney, New South Wales, Australia. ⁴Crown Princess Mary Cancer Centre Westmead Hospital, Westmead, New South Wales, Australia. ⁵Departments of Biomedical Sciences and Clinical Medicine, Faculty of Medicine and Health Sciences, Macquarie University, Sydney, New South Wales, Australia. ⁶Genentech, Inc., South San Francisco, California. ⁷Westmead Institute for Medical Research, University of Sydney, New South Wales, Australia. ⁸Vanderbilt University Medical Center, Nashville, Tennessee. ⁹The University of Texas MD Anderson Cancer Center, Houston, Texas. ¹⁰Royal Prince Alfred Hospital, Sydney, New South Wales, Australia. ¹¹Royal North Shore and Mater Hospitals, Sydney, New South Wales, Australia.

Note: Supplementary data for this article are available at Clinical Cancer Research Online (<http://clincancerres.aacrjournals.org/>).

Corresponding Author: Alexander M. Menzies, Melanoma Institute Australia, The University of Sydney and Royal North Shore and Mater Hospitals, 40 Rocklands Rd, North Sydney, NSW 2060, Australia. Phone: 612-9911-7200; Fax: 612-9954-9435; E-mail: alexander.menzies@sydney.edu.au

doi: 10.1158/1078-0432.CCR-18-1680

©2019 American Association for Cancer Research.

Translational Relevance

This study demonstrates that V600E and V600K *BRAF*-mutant melanomas are biologically distinct subtypes, not only having different clinical phenotypes, but also having different molecular features and differing responses to systemic therapies. V600K melanomas, most frequent in older patients with chronic sun damage, have less activation of the ERK pathway than V600E melanomas, what might explain their potential lower benefit with *BRAF*^{-/+}*MEKi* inhibitors, but in contrast, they have a higher mutational load and respond better to immunotherapy. The differences in gene expression and mutational load between V600E and V600K *BRAF*-mutant melanomas provide mechanistic data that translate to clinically significant differences in response to *BRAF*^{-/+}*MEKi* inhibitors and immunotherapy. Such findings should lead to the development of alternative treatment approaches for specific subtypes of *BRAF*-mutant melanoma.

progression-free survival (PFS) with *BRAF*^{-/+} compared with V600E melanomas, and two pooled analyses of *BRAF*[±]*MEKi* showed shorter PFS in multivariate analysis (10–15). As far as we are aware, there are no published data on the potential mechanisms responsible for these features, nor whether the *BRAF*-mutant genotype influences response to immunotherapy.

In this study, we sought to identify potential mechanisms for these apparent clinicopathologic differences, by comparing gene expression and mutational profiles of V600E and V600K melanomas from patients treated with *BRAF*[±]*MEKi*, validated on the Skin Cutaneous Melanoma (SKCM) The Cancer Genome Atlas (TCGA) dataset. We also explored whether the specific *BRAF*-mutant genotype affects response to immunotherapy.

Materials and Methods

Patients and outcome

Consecutive patients with V600E/K *BRAF*-mutant metastatic melanoma enrolled on clinical trials of *BRAF*[±]*MEK* inhibitors at two Melanoma Institute Australia treatment facilities (The Poche Centre, North Sydney, and Westmead Hospital—ethical approval from the Sydney Local Health District Human Research Ethics Committee, Protocol Number X15-0454 and HREC/11/RPAH/444) between July 2009 and July 2013 were included (*BRAF*[±]*MEKi* cohort; refs. 2, 3, 12, 13, 16–18). This study was conducted in accordance with the Declaration of Helsinki, and written-informed consent was obtained from all patients. Demographic and clinical data at the time of *BRAF*[±]*MEKi* treatment commencement were recorded for each patient, including gender, age, mutation status, lactate dehydrogenase (LDH) level, Eastern Cooperative Oncology Group (ECOG) performance status (PS), American Joint Committee on Cancer (AJCC) v.7 M-stage, and treatment (*BRAF*[±]*MEKi*). RECIST response, PFS and overall survival (OS) data were collected prospectively (data cut November 2016). An independent cohort of V600E/K *BRAF*-mutant metastatic melanoma patients treated with anti-PD-1 immunotherapy (pembrolizumab or nivolumab) was examined to explore response to anti-PD-1 immunotherapy by genotype (Immunotherapy cohort; ref. 19).

Tumor samples and molecular testing

Tumor genomic DNA and RNA were extracted from formalin-fixed, paraffin-embedded (FFPE) melanoma tissue pretreatment samples from the 93 patients (*BRAF*[±]*MEKi* cohort). Two samples were from primary melanomas, 25 were from lymph nodes, and the remaining 66 were from distant metastatic sites. Samples were macrodissected prior to nucleic acid extraction. DNA was extracted using QIAamp DNA FFPE Tissue Kit (Qiagen, #56404), and RNA was extracted using the High Pure RNA Micro Kit (Roche, #04823125001).

NanoString RNA gene expression analysis. A custom-designed NanoString panel of 814 probes was used (Supplementary Table S1). Of these, 5 genes (*HPRT1*, *GUSB*, *CLTC*, *PGK1*, and *SDHA*) were built-in as housekeeping genes, 8 probes were negative controls, and 6 were positive controls. All samples had mutant *BRAF* detected with adequate quality. Expression data were imported and normalized by the NanoStringQCPro package, following the manufacturer's recommendations (20).

Next-generation DNA sequencing. A pan-cancer 88-gene next-generation sequencing (NGS) panel to detect DNA coding mutations was performed on all 93 samples as has been previously described (21). Briefly, 963 amplicons targeting 88 genes were enriched for by Access Array (Fluidigm) and sequenced (2 × 108 bp). FASTQ reads were aligned to the human reference genome (NCBI Build 37) using GSNAP (22, 23). Duplicate reads in the resulting BAM file were marked using PicardTools, and indels realigned using the GATK IndelRealigner tool. The median sequencing depth was 2,822x (range, 4–3,415x), and a minimum of 150x was required for analysis. Synonymous coding mutations (as defined by Ensembl) were discarded, and mutational load was calculated as number of mutations per sample (Supplementary Table S2).

TCGA data. TCGA SKCM (24) RNA sequencing (RNA-seq) and whole-exome sequencing (WES) datasets for *BRAF* V600E ($N = 116$) and V600K ($n = 17$) samples were downloaded on February 6, 2017, using R package TCGAbiolinks (25) from the GDC portal. All alignments were performed using the human reference genome GRCh38.d1.vd1. Aligned and cocleaned BAM files were processed through the Somatic Mutation Calling Workflow as tumor-normal pairs. Variant calling was performed using the mutect2 (26) pipeline. Synonymous variants were discarded and then mutational load was calculated as number of mutations per sample. Samples with more than 2,000 mutations were filtered out, and a Mann-Whitney test was performed between V600E and V600K samples. Raw RNA-seq read count data were downloaded with the option HTSeq-count. Genes with less than 20 counts were filtered out.

Statistical methods

Gene expression analysis. On both the NanoString platform and the TCGA data (27), a differential expression analysis was performed between the V600E and V600K cohorts, and a gene was defined as differentially expressed when its FDR-adjusted P value was less than 0.05. On the NanoString platform, the differential analysis was performed using a moderated t test implemented in the R (28) package limma (29), and on the TCGA data, the differential analysis was performed on raw counts using a negative binomial model and the associated Wald significant test implemented in the DESeq2 package (30).

On both the TCGA and the NGS datasets, the Mann–Whitney *U* test was performed to compare the mutational load between V600E and V600K samples. Statistical significance was defined by *P* value less than 0.05. Visualization of genes expression levels and subsequent pathway analysis used log-transformed fragments per kilobase million (FPKM) value.

Gene set enrichment analysis. Selected genesets were downloaded from Molecular Signatures Database (MSigDB) version 6.0. We created a ERK pathway gene set by using 12 genes common to the two expert-derived Pratilas (31) and Nazarian (32) gene sets. A PI3K-AKT pathway gene set was compiled by using 112 genes common to the AKT_UP.V1_UP and AKT_UP_MTOR_DN.V1_UP genesets in MSigDB (33, 34). To determine the significance of a pathway, a Hotelling T2 test with a shrinkage estimator was used based on implementation in the Hotelling package (35).

Survival analysis. Kaplan–Meier plots and the log-rank test implemented in the survival package (36) in R were used for survival analysis.

Results

Patient characteristics (*BRAF*ⁱ±*MEK*ⁱ cohort)

Ninety-three consecutive patients with V600E (*n* = 78) or V600K (*n* = 15) *BRAF*-mutant metastatic melanoma treated with *BRAF*ⁱ±*MEK*ⁱ on clinical trials at two Melanoma Institute Australia treatment facilities (The Poche Centre, North Sydney and Westmead Hospital) were examined (Table 1). The cohort was typical for a metastatic melanoma clinical trial population, and there were no statistical differences between genotypes (Table 1). Although not statistically different, likely due to small sample size for the V600K group, the median age was numerically higher in V600K compared with V600E melanoma patients (median, 58 vs. 56.5 years old). Forty percent of patients in both groups had an ECOG PS ≥ 1, 80% had AJCC M1c disease, and LDH was elevated in 27% (V600E) and 40% (V600K) of patients. Only 20% of the V600E patients were treated with combination *BRAF*+*MEK* inhibitors, whereas 33% of the V600K patients were treated with combination therapy.

Table 1. Baseline characteristics of patients with V600E versus V600K metastatic melanoma (*BRAF*ⁱ±*MEK*ⁱ cohort)

Characteristics	V600E (<i>n</i> = 78)	V600K (<i>n</i> = 15)	<i>P</i> value
Age (years)			
Median	56.5	58.0	0.418
Gender (<i>N</i> , %)			0.5786
Female	33 (42%)	5 (33%)	
Male	45 (58%)	10 (67%)	
AJCC stage ^a (<i>N</i> , %)			1
IIIC–M1b	19 (24%)	3 (20%)	
M1c	59 (76%)	12 (80%)	
LDH (<i>N</i> , %)			0.3563
Normal	57 (73%)	9 (60%)	
Elevated	21 (27%)	6 (40%)	
ECOG (<i>N</i> , %)			1
0	47 (60%)	9 (60%)	
≥1	31 (40%)	6 (40%)	
Treatment (<i>N</i> , %)			0.3162
<i>BRAF</i> ⁱ	62 (80%)	10 (67%)	
<i>BRAF</i> ⁱ + <i>MEK</i> ⁱ	16 (20%)	5 (33%)	

^aAJCC v7 anatomic staging, excluding LDH and brain metastases.

V600K melanomas have inferior response and PFS with *BRAF*ⁱ±*MEK*ⁱ, compared with V600E melanomas

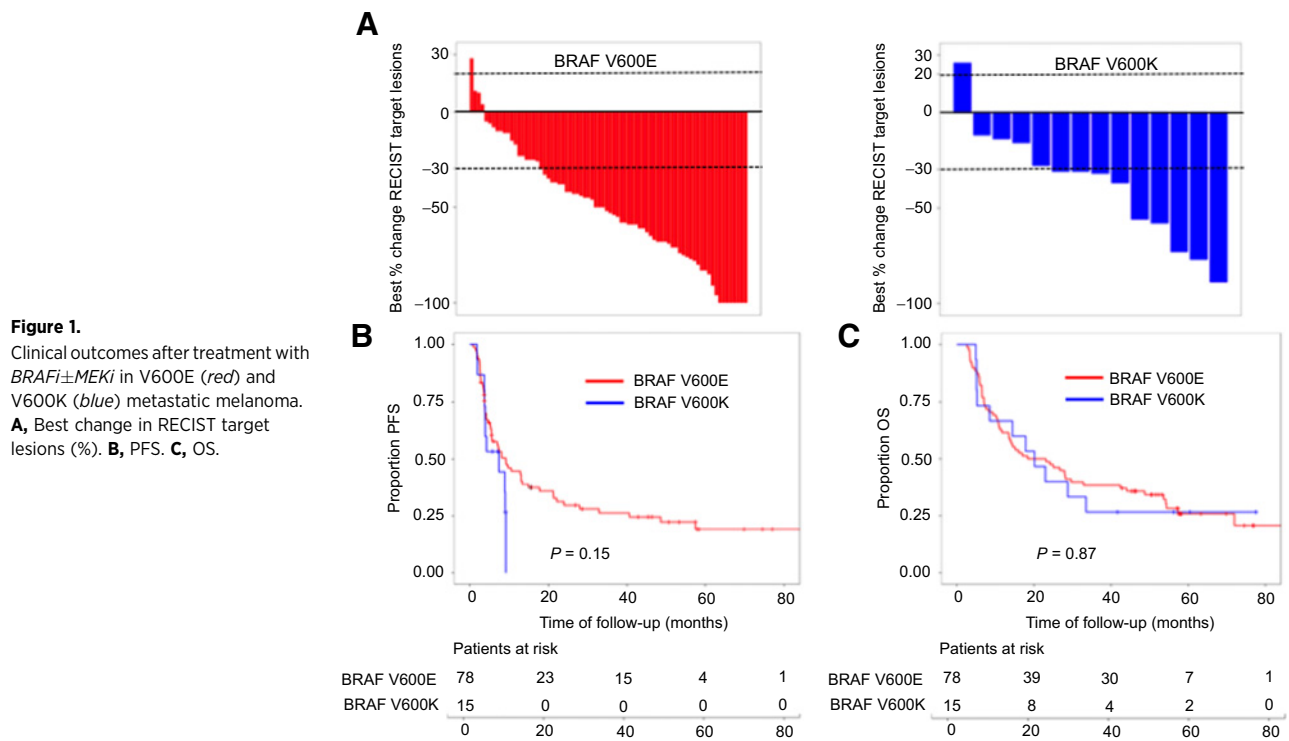
Few direct comparisons of response rates and survival between V600E and V600K melanomas have been performed previously; however, phase III clinical trials and two pooled analyses suggest that V600K melanomas may have a lower response rate and shorter PFS with *BRAF*ⁱ±*MEK*ⁱ compared with V600E melanomas, and yet have similar OS (10–15). In this study, which included a small number of V600K melanomas, despite the fact more patients with V600K melanoma were treated with combination *BRAF*+*MEK* inhibitors, patients with V600K melanoma had a numerically lower median degree of response to therapy (–31% vs. –52%, *P* = 0.15) and a lower rate of complete response (0% vs. 10%; Fig. 1A). Although not statistically significant, V600K patients also had a median PFS of 5.7 months, and no patient remained progression-free beyond 9 months, whereas median PFS was 7.1 months in V600E patients, and approximately 20% remained progression-free at 5 years (Fig. 1B). Despite these numerical differences in response rates and PFS, OS was similar (Fig. 1C).

V600K melanomas have less ERK but more PI3K pathway activation

To investigate potential mechanisms for these clinicopathologic differences, including a possible smaller benefit with *BRAF*ⁱ±*MEK*ⁱ in V600K melanomas, we sought to identify differences in gene expression between both groups. Nanostring data revealed that expression of dual-specificity phosphatase 6 (*DUSP6*), a transcriptional target of the ERK pathway involved in feedback regulation and reflective of ERK activation, was the most significantly differentiated gene, with lower expression in V600K melanoma (*P* = 0.024, Fig. 2A). This was confirmed using RNA-seq data from the TCGA, including V600E (*n* = 116) and V600K (*n* = 17) tumors (*n* = 133, *P* = 0.003; Fig. 2B). Moreover, besides *DUSP6*, other genes related to transcriptional output of MEK/ERK pathway including *ETV4*, *DUSP4*, and *SPRY2* were within the top 30 differentially expressed genes, with higher expression in V600E melanomas, whereas *PIK3CB* expression was higher in V600K melanomas (Supplementary Table S1). We then performed pathway analyses assessing the expression of ERK and PI3K (an alternative survival pathway) pathway gene set signatures using the TCGA dataset. Interestingly, the expression of ERK pathway genes was lower in V600K melanomas (*P* = 0.0003), whereas the expression of PI3K–AKT pathway genes was significantly higher in V600K melanoma compared with V600E (*P* = 0.005; Supplementary Fig. S1). These data support the hypothesis that V600K melanomas are less dependent on the ERK pathway and more dependent on alternative pathways, specifically the PI3K–AKT pathway.

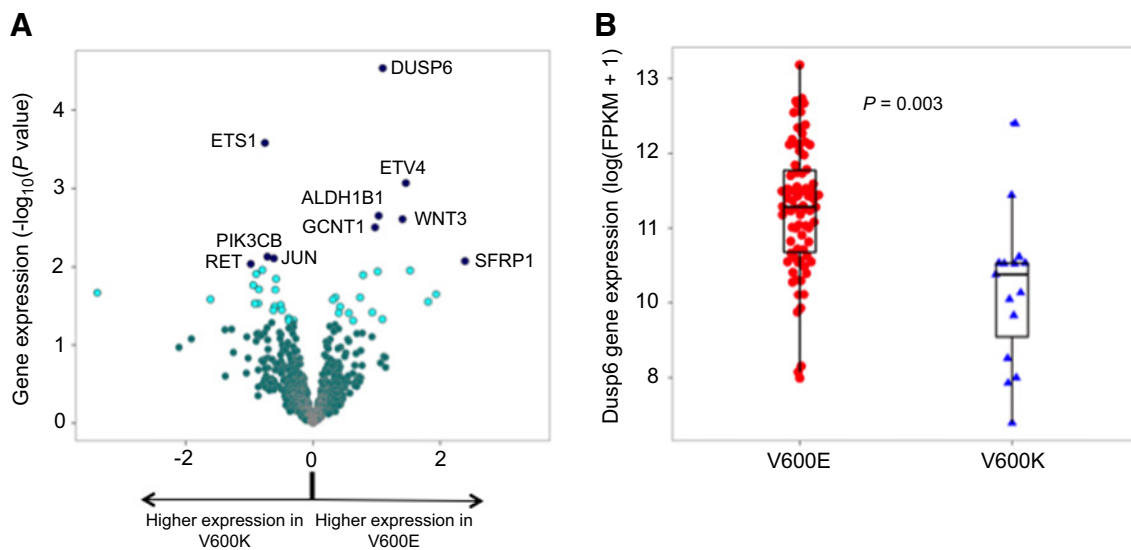
V600K melanomas have a higher mutational load

In an attempt to explore whether mutational data may explain differences in both pathway expression and the clinical phenotype of V600E and V600K melanoma, targeted NGS data of genomic DNA were examined. As expected given the clinical phenotype, V600K melanomas had a numerically but insignificantly higher mutational load in our *BRAF*ⁱ±*MEK*ⁱ cohort using the 88-gene panel (*P* = 0.1375; Fig. 3A); however, WES data from the TCGA cohort revealed a significantly higher mutational load in V600K melanomas (*P* = 0.0003; Fig. 3B). The genes that were more frequently mutated in V600K melanoma on NGS fitted mainly



into three groups: PI3K–AKT pathway genes (*PIK3R1*), tumor-suppressor genes (*SMARCA4*, *NF2*, *RB1*, *FBXW7*, *TP53*, and *APC*), and proto-oncogenes (*KIT*, *RET*, and *KRAS*; Supplementary Fig. S2; Supplementary Table S2). In the TCGA dataset, however, the

frequency of mutations in these genes was very low, precluding further conclusions (Supplementary Fig. S3). Given prior associations with mutational load, immune expression, and immunotherapy response, we then looked at the expression of immune



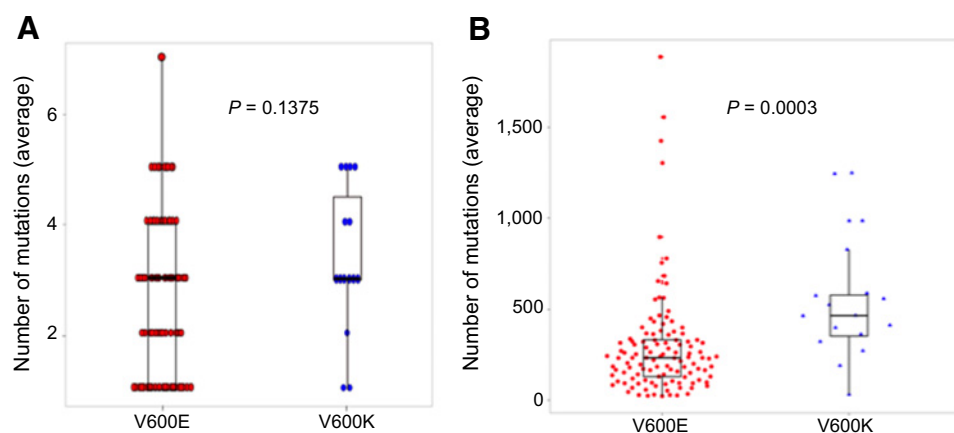


Figure 3. Mutational load in V600E (red) and V600K (blue) melanoma. NGS data from *BRAFi±MEKi* cohort (A) and TCGA (B) data. Each dot/triangle represents one single sample.

genes, by checking iPRES signature (37) in V600E- versus V600K-mutant melanoma in the TCGA dataset, but no significant difference was detected between these two genotypes (Supplementary Fig. S4). We further explored whether there was a subset of V600E melanomas that behave like V600K melanomas. Analyses of *DUSP6* expression, mutational load, age, and response to therapy did not identify a clear subset of V600E melanomas behaving like V600K melanoma, that is, having lower *DUSP6* expression, with higher mutation burden, in older patients with less response to *BRAFi±MEKi* (Supplementary Fig. S5).

V600K melanomas have superior response and survival with immunotherapy

Finally, based on the higher mutational load seen in V600K melanomas, we hypothesized that they should respond better to immunotherapy than V600E melanoma. We examined an independent cohort of 103 *BRAF* V600E/K patients treated with anti-PD-1 immunotherapy (V600E, $n = 84$; V600K, $n = 19$; ref. 19; Table 2). Patients with V600K were significantly older than those with V600E melanoma (61.5 vs. 50 years old,

$P = 0.0358$) and were more often male (84% vs. 51%, $P = 0.01$; Table 2). No significant difference was found between groups regarding known prognostic factors including AJCC stage, LDH level, or ECOG PS, and a similar percentage of patients from both groups had received prior treatment with *BRAFi±MEKi* (42% vs. 44%, $P = 0.8042$). With a median 31.7-month follow-up, there was a trend toward a higher response rate to immunotherapy in patients with V600K compared with V600E melanomas (53% vs. 29%, $P = 0.059$; Fig. 4A). Moreover, PFS was longer in V600K melanoma patients (median, 19 vs. 2.7 months, $P = 0.049$; Fig. 4B), whereas the prolonged OS for V600K did not reach statistical significance (20.4 vs. 11.7 months, $P = 0.081$; Fig. 4C).

Discussion

This study demonstrates that V600E and V600K *BRAF*-mutant melanomas are biologically distinct subtypes of melanoma, not only having different clinical phenotypes, but also having different molecular features and differing responses to systemic therapies. V600K melanomas, most frequent in older patients with chronic sun damage, have less activation of the ERK pathway than V600E melanomas, potentially explaining their relative resistance to *BRAFi±MEKi*, but in contrast, they have a higher mutational load and respond better to immunotherapy.

BRAF is a serine/threonine protein kinase that activates the ERK signaling pathway (38). *BRAF* V600 mutations induce RAS-independent activation of the ERK pathway, with consequent dysregulation of ERK signaling (high expression and activation of ERK), driving cell proliferation, and survival (39). Moreover, the normal feedback regulation through the Sprouty and *DUSP* families is insufficient to downregulate pathway activation in the presence of constitutively activated *BRAF* (40). In this study, we demonstrated in pretreatment biopsies from melanoma patients that the negative feedback regulator of the ERK pathway, *DUSP6* (41), is expressed higher in V600E melanomas compared with V600K. This relative increase in ERK pathway activation, confirmed using gene set expression analysis from the TCGA dataset, is consistent with cell line data demonstrating higher fold *BRAF*-kinase activity in V600E-mutant cell lines compared with V600K (42). Furthermore, we demonstrated that an alternative proliferation and survival pathway, the PI3K-AKT pathway, is more activated in V600K melanoma. Together, these data suggest differential

Table 2. Baseline characteristics of patients with V600E versus V600K metastatic melanoma (immunotherapy cohort)

Characteristics	V600E (n = 84)	V600K (n = 19)	P value
Age (years)			
Median	51	61.5	0.0358
Gender (N, %)			0.001
Female	41 (49%)	3 (16%)	
Male	43 (51%)	16 (84%)	
AJCC stage ^a (N, %)			0.7571
IIIC-MIb	18 (21%)	3 (16%)	
MIc	66 (79%)	16 (84%)	
LDH (N, %)			0.1195
Normal	49 (58%)	15 (79%)	
Elevated	35 (42%)	4 (21%)	
ECOG (N, %)			0.2037
0	42 (50%)	13 (68%)	
≥1	42 (50%)	6 (32%)	
Prior MAPKi (N, %)			0.8042
No	47 (56%)	11 (58%)	
Yes	37 (44%)	8 (42%)	
PD1 therapy (N, %)			0.0229
Nivolumab	22	2	
Pembrolizumab	62	17	

^aAJCC v7 anatomic staging, excluding LDH and brain metastases.

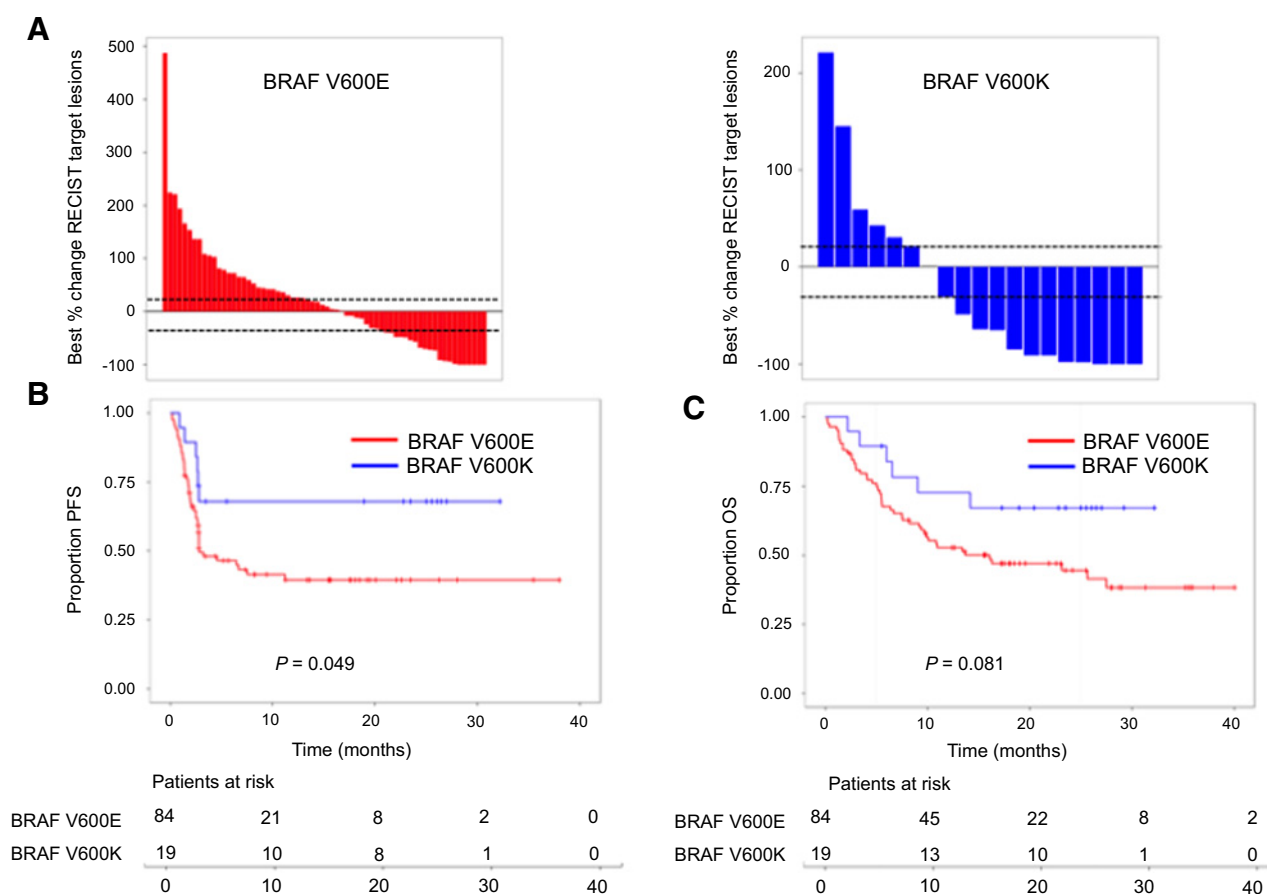


Figure 4.

Clinical outcomes after treatment with anti-PD-1 immunotherapy in V600E (red) and V600K (blue) metastatic melanoma. **A**, Best change in RECIST targets (%). **B**, PFS. **C**, OS.

activity of pathway signaling in V600E and V600K melanomas, potentially explaining the relative resistance of V600K melanoma to *BRAF* \pm *MEK* despite similar potency for inhibition with dabrafenib (IC_{50} , 0.65 V600E and 0.5 V600K, respectively; ref. 43). This possible disadvantage of V600K melanoma with *BRAF* \pm *MEK* may be seen in the clinic, with this dataset as well as clinical trials suggesting that V600K patients have lower response rate and shorter PFS compared with V600E patients (10–15). Few direct comparisons have been performed in large datasets from clinical trials, and given the small V600K sample size in the study, results require validation in larger studies.

Although V600 *BRAF*-mutant melanomas typically occur in younger patients whose tumors arise on skin without chronic sun-induced damage (5), these associations are driven by the V600E genotype, which is the most frequent (70%–80% *BRAF*-mutant melanomas). In contrast, V600K melanomas (20%–30%) typically occur in older patients, on the head and neck, and in chronic sun-damaged skin (8). Consistent with these clinicopathologic differences, our data demonstrate a higher mutational load in V600K melanomas, and that several groups of genes, notably tumor-suppressor genes and proto-oncogenes, are more frequently mutated in this genotype. Our data also show that *BRAF*V600K

melanomas respond significantly better than V600E melanomas to anti-PD-1 immunotherapy, with a higher response rate, and longer PFS and OS. Such results are consistent with several studies that have shown an association with tumor mutational load and response to immunotherapy (44, 45), but confirmation of these clinical findings should be validated in larger cohorts, such as a *post hoc* analysis of the CheckMate-067 and Keynote-006 clinical trials (46, 47).

Despite the large number of melanoma tissue samples, a limitation of this study is the size of the V600K cohort, which diminished the power to analyze associations between the molecular findings and clinical outcomes. This limitation could explain the lack of significant difference in the expression of immune markers between these two genotypes. We did not see a difference in the expression of immune markers in TCGA cohort either, as differently from our *BRAF* \pm *MEK* cohort where we have macro-dissected the tumors, TCGA analyzed the highest tumor content areas, and may have missed the tumor–stroma interface. Limited DNA sequencing and RNA expression panels were run from FFPE tumors, with less data obtained than that gained from whole exome/genome and RNA sequencing studies in fresh-frozen tumors. Such data were available in the TCGA cohort, however,

and validation of our FFPE-based molecular data using a similarly size TCGA dataset strengthens the findings of this study. Prospective samples from stage III and IV patients have been collected in order to further characterize immune signatures and correlate these with response to immunotherapy in the adjuvant and metastatic settings, and the respective mutant *BRAF* genotype.

For patients with *BRAF*-mutant metastatic melanoma, the selection of therapy to give the highest chance of long-term durable control, either immunotherapy or targeted therapy, remains a challenge. There are no trial data to suggest the most appropriate sequence, and there are no biomarkers that can accurately identify patients likely to derive long-term benefit with either treatment. This is now also a dilemma in the adjuvant setting (4, 48, 49). Our data, along with the published *BRAF*±*MEKi* clinical trials, suggest that V600K melanomas may be best served with adjuvant immunotherapy. In addition to exploring clinical trial data in the metastatic setting, data from the adjuvant clinical trials should also be explored by *BRAF* mutation genotype (4, 48, 49). If our results are validated, the best treatment for patients with *BRAF*-mutant melanoma may well differ based on V600E and V600K genotypes.

The differences in gene expression and mutational load between V600E and V600K *BRAF*-mutant melanomas provide translational data that explain clinically meaningful differences in response to *BRAF*±*MEKi* and immunotherapy, and provide further rationale for the selection of one therapy over the other. Such findings should lead to the development of alternative treatment approaches for specific genotypes of *BRAF*-mutant melanoma.

Disclosure of Potential Conflicts of Interest

J. Holst is an employee of and reports receiving other commercial research support from MetaboloQ Pharmaceuticals. M.S. Carlino is a consultant/advisory board member for Bristol-Myers Squibb, MSD, Novartis, Amgen, and Pierre-Fabre. M. Wongchenko holds ownership interest (including patents) in Roche and Ariad Pharmaceuticals. Y. Yan holds ownership interest (including patents) in Genentech. D.B. Johnson reports receiving commercial research grants from Bristol-Myers Squibb and Incyte, and is a consultant/advisory board member for Array, Bristol-Myers Squibb, Genoptix, Incyte, and Merck. R.F. Kefford is a consultant/advisory board member for Amgen and reports receiving other remuneration in the form of conference expenses from Bristol-Myers Squibb and Amgen. R.A. Scolyer is a consultant/advisory board member for Merck Sharp & Dohme and Novartis. G.V. Long is a consultant/advisory board member for Bristol-Myers Squibb, Novartis, Roche, Amgen, Pierre-Fabre, Array, and Merck. A.M. Menzies is a consultant/advisory board member for Bristol-

Myers Squibb, MSD, Novartis, Roche, and Pierre-Fabre. No potential conflicts of interest were disclosed by the other authors.

Authors' Contributions

Conception and design: I. Pires da Silva, M.S. Carlino, Y. Yan, D.B. Johnson, R.A. Scolyer, A.M. Menzies

Development of methodology: I. Pires da Silva, J.J. Park, Y. Yan, R.A. Scolyer, A.M. Menzies

Acquisition of data (provided animals, acquired and managed patients, provided facilities, etc.): I. Pires da Silva, J.S. Wilmott, M.S. Carlino, J.J. Park, M. Wongchenko, Y. Yan, G. Mann, D.B. Johnson, J.L. McQuade, R. Rai, R.F. Kefford, R.A. Scolyer, G.V. Long, A.M. Menzies

Analysis and interpretation of data (e.g., statistical analysis, biostatistics, computational analysis): I. Pires da Silva, K.Y.X. Wang, J. Holst, J.J. Park, C. Quek, M. Wongchenko, Y. Yan, H. Rizos, R.A. Scolyer, J.Y.H. Yang, G.V. Long, A.M. Menzies

Writing, review, and/or revision of the manuscript: I. Pires da Silva, K.Y.X. Wang, J.S. Wilmott, J. Holst, M.S. Carlino, J.J. Park, C. Quek, M. Wongchenko, Y. Yan, G. Mann, D.B. Johnson, J.L. McQuade, R.F. Kefford, H. Rizos, R.A. Scolyer, J.Y.H. Yang, G.V. Long, A.M. Menzies

Administrative, technical, or material support (i.e., reporting or organizing data, constructing databases): I. Pires da Silva, J.S. Wilmott, C. Quek, G. Mann, A.M. Menzies

Study supervision: J.S. Wilmott, R.A. Scolyer, A.M. Menzies

Acknowledgments

The authors are thankful for the assistance of Jess Hyman, Hazel Burke, Alex Guminski, and Raghwa Sharma. J.S. Wilmott is supported by an NHMRC Research Fellowship. J.L. McQuade is supported by an ASCO/CCF Career Development Award, a Melanoma SPORE Developmental Research Program Award, and an NIH T32 Training Grant CA009666. R.A. Scolyer is supported by an NHMRC Practitioner Fellowship. J.Y.H. Yang is supported by NHMRC CDF and ARC Discovery Project grant (DP170100654). G.V. Long is supported by an NHMRC Practitioner Fellowship and the University of Sydney Medical Foundation. A.M. Menzies is supported by a Cancer Institute NSW Fellowship. This work was supported by a Pfizer Australia grant (WS2345795 to A.M. Menzies), and a Cancer Council NSW grant (RG17-04 to J. Holst, J.S. Wilmott, and A.M. Menzies). This research was also supported by an Australian National Health and Medical Research Council program grant. Assistance from other colleagues at Melanoma Institute Australia and the Royal Prince Alfred Hospital is also gratefully acknowledged.

The costs of publication of this article were defrayed in part by the payment of page charges. This article must therefore be hereby marked *advertisement* in accordance with 18 U.S.C. Section 1734 solely to indicate this fact.

Received June 11, 2018; revised September 12, 2018; accepted November 1, 2018; published first January 10, 2019.

References

- Hodis E, Watson IR, Kryukov GV, Arold ST, Imielinski M, Theurillat JP, et al. A landscape of driver mutations in melanoma. *Cell* 2012;150:251–63.
- Chapman PB, Hauschild A, Robert C, Haanen JB, Ascierto P, Larkin J, et al. Improved survival with vemurafenib in melanoma with BRAF V600E mutation. *N Engl J Med* 2011;364:2507–16.
- Hauschild A, Grob JJ, Demidov LV, Jouary T, Gutzmer R, Millward M, et al. Dabrafenib in BRAF-mutated metastatic melanoma: a multicentre, open-label, phase 3 randomised controlled trial. *Lancet* 2012;380:358–65.
- Long GV, Hauschild A, Santinami M, Atkinson V, Mandalà M, Chiarion-Sileni V, et al. Adjuvant dabrafenib plus trametinib in stage III BRAF-mutated melanoma. *N Engl J Med* 2017;377:1813–23.
- Ascierto PA, Kirkwood JM, Grob JJ, Simeone E, Grimaldi AM, Maio M, et al. The role of BRAF V600 mutation in melanoma. *J Transl Med* 2012;10:85.
- Long GV, Menzies AM, Nagrial AM, Haydu LE, Hamilton AL, Mann GJ, et al. Prognostic and clinicopathologic associations of oncogenic BRAF in metastatic melanoma. *J Clin Oncol* 2011;29:1239–46.
- Lyle M, Haydu LE, Menzies AM, Thompson JF, Saw RP, Spillane AJ, et al. The molecular profile of metastatic melanoma in Australia. *Pathology* 2016;48:188–93.
- Menzies AM, Haydu LE, Visintin L, Carlino MS, Howle JR, Thompson JF, et al. Distinguishing clinicopathologic features of patients with V600E and V600K BRAF-mutant metastatic melanoma. *Clin Cancer Res* 2012;18:3242–9.
- Buchheit AD, Syklawer E, Jakob JA, Bassett RL Jr, Curry JL, Gershenwald JE, et al. Clinical characteristics and outcomes with specific BRAF and NRAS mutations in patients with metastatic melanoma. *Cancer* 2013;119:3821–9.
- McArthur GA, Chapman PB, Robert C, Larkin J, Haanen JB, Dummer R, et al. Safety and efficacy of vemurafenib in BRAF(V600E) and BRAF(V600K) mutation-positive melanoma (BRIM-3): extended follow-up of a phase 3, randomised, open-label study. *Lancet Oncol* 2014;15:323–32.
- Larkin J, Ascierto PA, Dréno B, Atkinson V, Lischkay G, Maio M, et al. Combined vemurafenib and cobimetinib in BRAF-mutated melanoma. *N Engl J Med* 2014;371:1867–76.

12. Robert C, Karaszewska B, Schachter J, Rutkowski P, Mackiewicz A, Stroiakovski D, et al. Improved overall survival in melanoma with combined dabrafenib and trametinib. *N Engl J Med* 2015;372:30–9.
13. Long GV, Stroyakovskiy D, Gogas H, Levchenko E, de Braud F, Larkin J, et al. Combined BRAF and MEK inhibition versus BRAF inhibition alone in melanoma. *N Engl J Med* 2014;371:1877–88.
14. Schadendorf D, Long GV, Stroiakovski D, Karaszewska B, Hauschild A, Levchenko E, et al. Three-year pooled analysis of factors associated with clinical outcomes across dabrafenib and trametinib combination therapy phase 3 randomised trials. *Eur J Cancer* 2017;82:45–55.
15. Long GV, Grob JJ, Nathan P, Ribas A, Robert C, Schadendorf D, et al. Factors predictive of response, disease progression, and overall survival after dabrafenib and trametinib combination treatment: a pooled analysis of individual patient data from randomised trials. *Lancet Oncol* 2016;17:1743–54.
16. Flaherty KT, Robert C, Hersey P, Nathan P, Garbe C, Milhem M, et al. Improved survival with MEK inhibition in BRAF-mutated melanoma. *N Engl J Med* 2012;367:107–14.
17. Long GV, Trefzer U, Davies MA, Kefford RF, Ascierto PA, Chapman PB, et al. Dabrafenib in patients with Val600Glu or Val600Lys BRAF-mutant melanoma metastatic to the brain (BREAK-MB): a multicentre, open-label, phase 2 trial. *Lancet Oncol* 2012;13:1087–95.
18. Ascierto PA, McArthur GA, Dréno B, Atkinson V, Liskay G, Di Giacomo AM, et al. Cobimetinib combined with vemurafenib in advanced BRAF (V600)-mutant melanoma (coBRIM): updated efficacy results from a randomised, double-blind, phase 3 trial. *Lancet Oncol* 2016;0:949–54.
19. Rai R, McQuade JL, Wang DY, Park JJ, Nahar K, Sosman JA, et al. Safety and efficacy of anti-PD-1 antibodies in elderly patients with metastatic melanoma. *Ann Oncol* 27:379–400.
20. Nickles D, Sandmann T, Ziman R, Bourgon R. NanoStringQCPro: Quality metrics and data processing methods for NanoString mRNA gene expression data. *R Packag version 1100*, 2017;1–9.
21. Bourgon R, Lu S, Yan Y, Lackner MR, Wang W, Weigman V, et al. High-throughput detection of clinically relevant mutations in archived tumor samples by multiplexed PCR and next-generation sequencing. *Clin Cancer Res* 2014;20:2080–91.
22. Wu TD, Nacu S. Fast and SNP-tolerant detection of complex variants and splicing in short reads. *Bioinformatics* 2010;26:873–81.
23. Wu TD, Reeder J, Lawrence M, Becker G, Brauer MJ. GMAP and GSNAP for genomic sequence alignment: Enhancements to speed, accuracy, and functionality. *Methods Mol Biol* 2016;1418:283–334.
24. Guan J, Gupta R, Filipp FV. Cancer systems biology of TCGA SKCM: efficient detection of genomic drivers in melanoma. *Sci Rep* 2015;5:7857.
25. Colaprico A, Silva TC, Olsen C, Garofano L, Cava C, Garolini D, et al. TCGAAbiolinks: an R/Bioconductor package for integrative analysis of TCGA data. *Nucleic Acids Res* 2016;44:e71.
26. Cibulskis K, Lawrence MS, Carter SL, Sivachenko A, Jaffe D, Sougnez C, et al. Sensitive detection of somatic point mutations in impure and heterogeneous cancer samples. *Nat Biotechnol* 2013;31:213–9.
27. Network TCGA. Genomic classification of cutaneous melanoma. *Cell* 2015;161:1681–96.
28. R Development Core Team. R: a language and environment for statistical computing. Vienna, Austria: R Foundation for Statistical Computing; 2017.
29. Ritchie ME, Phipson B, Wu D, Hu Y, Law CW, Shi W, et al. limma powers differential expression analyses for RNA-sequencing and microarray studies. *Nucleic Acids Res* 2015;43:e47.
30. Love MI, Huber W, Anders S. Moderated estimation of fold change and dispersion for RNA-seq data with DESeq2. *Genome Biol* 2014;15:550.
31. Pratilas CA, Taylor BS, Ye Q, Viale A, Sander C, Solit DB, et al. V600EBRAF is associated with disabled feedback inhibition of RAF-MEK signaling and elevated transcriptional output of the pathway. *Proc Natl Acad Sci U S A* 2009;106:4519–24.
32. Nazarian R, Shi H, Wang Q, Kong X, Koya RC, Lee H, et al. Melanomas acquire resistance to B-RAF(V600E) inhibition by RTK or N-RAS upregulation. *Nature* 2010;468:973–7.
33. Subramanian A, Tamayo P, Mootha VK, Mukherjee S, Ebert BL, Gillette MA, et al. Gene set enrichment analysis: a knowledge-based approach for interpreting genome-wide expression profiles. *Proc Natl Acad Sci U S A* 2005;102:15545–50.
34. Hugo W, Birger C, Thorvaldsdóttir H, Ghandi M, Mesirov JP, Tamayo P. The molecular signatures database hallmark gene set collection. *Cell Syst* 2015;1:417–25.
35. Curran J (2017). Hotelling: hotelling's T² test and variants. Version 1.0–5, <http://www.stat.auckland.ac.nz/showperson?firstname=James&surname=Curran>.
36. Therneau T (2015). A Package for Survival Analysis in S. version 2.38, <https://CRAN.R-project.org/package=survival>.
37. Hugo W, Zaretsky JM, Sun L, Song C, Moreno BH, Hu-Lieskovan S, et al. Genomic and transcriptomic features of response to anti-PD-1 therapy in metastatic melanoma. *Cell* 2016;165:35–44.
38. Dhillion AS, Hagan S, Rath O, Kolch W. MAP kinase signalling pathways in cancer. *Oncogene* 2007;26:3279–90.
39. Poulidakos PI, Rosen N. Mutant BRAF melanomas-dependence and resistance. *Cancer Cell* 2011;19:11–5.
40. Montero-Conde C, Ruiz-Llorente S, Dominguez JM, Knauf JA, Viale A, Sherman EJ, et al. Relief of feedback inhibition of HER3 transcription by RAF and MEK inhibitors attenuates their antitumor effects in BRAF-mutant thyroid carcinomas. *Cancer Discov* 2013;3:520–33.
41. Kidger AM, Keyse SM. The regulation of oncogenic Ras/ERK signalling by dual-specificity mitogen activated protein kinase phosphatases (MKPs). *Semin Cell Dev Biol* 2016;50:125–32.
42. Wan PTC, Garnett MJ, Roe SM, Lee S, Niculescu-Duvaz D, Good VM, et al. Mechanism of activation of the RAF-ERK signaling pathway by oncogenic mutations of B-RAF. *Cell* 2004;116:855–67.
43. Menzies AM, Long GV, Murali R. Dabrafenib and its potential for the treatment of metastatic melanoma. *Drug Des Devel Ther* 2012;6:391–405.
44. Snyder A, Makarov V, Merghoub T, Yuan J, Zaretsky JM, Desrichard A, et al. Genetic basis for clinical response to CTLA-4 blockade in melanoma. *N Engl J Med* 2014;371:2189–99.
45. Danilova L, Wang H, Sunshine J, Kaunitz GJ, Cottrell TR, Xu H, et al. Association of PD-1/PD-L axis expression with cytolytic activity, mutational load, and prognosis in melanoma and other solid tumors. *Proc Natl Acad Sci U S A* 2016;113:E7769–77.
46. Wolchok JD, Kluger H, Callahan MK, Postow MA, Rizvi NA, Lesokhin AM, et al. Nivolumab plus ipilimumab in advanced melanoma. *N Engl J Med* 2013;369:122–33.
47. Robert C, Schachter J, Long GV, Arance A, Grob JJ, Mortier L, et al. Pembrolizumab versus ipilimumab in advanced melanoma. *N Engl J Med* 2015;372:2521–32.
48. Weber J, Mandala M, Del Vecchio M, Gogas HJ, Arance AM, Cowey CL, et al. Adjuvant nivolumab versus ipilimumab in resected stage III or IV melanoma. *N Engl J Med* 2017;377:1824–35.
49. Eggermont AMM, Blank CU, Mandala M, Long GV, Atkinson V, Dalle S, et al. Adjuvant pembrolizumab versus placebo in resected stage III melanoma. *N Engl J Med* 2018;378:1789–801.